

## Article

# Plasma Technology Applied to Improve Wettability for Emerging Mycelium-Based Materials

Paz Aragón Chivite <sup>\*</sup>, Núria Portolés Gil, Ruth Garcia Campà , Lorenzo Bautista Pérez   
and Paula Félix de Castro

Applied Chemistry and Materials Department, Applied Research and Technology Services, Leitat Technological Center, 08225 Terrassa, Spain; nportoles@leitat.org (N.P.G.); rgarcia@leitat.org (R.G.C.); lbautista@leitat.org (L.B.P.); pfelix@leitat.org (P.F.d.C.)

\* Correspondence: paragon@leitat.org

**Abstract:** Plasma technology is increasing its applications in the textile industry for conferring surface functionalities through greener processes. In this study, plasma treatments are studied to improve the wettability of mycelium-based material, an emerging material with a lot of potential in the near future. The plasma effect was characterized by assessing the added functionality (wettability) and inspecting surface modifications with different techniques, such as scanning electron microscopy (SEM) and X-Ray photoelectron spectroscopy (XPS). Low pressure plasma (LPP) treatments were successfully applied into the mycelium-based material and optimal power of discharge and treatment time were set for this material (750 W, 17.5 min). With the optimized LPP treatments, the water absorption capacity of mycelium-based material was improved by 2000% and some surface morphological modifications were observed by SEM analysis. On the other hand, XPS analysis demonstrated how the plasma treatment changes the surface composition.

**Keywords:** low pressure plasma; surface modification; mycelium; textile finishing; water absorption; wettability



**Citation:** Aragón Chivite, P.; Portolés Gil, N.; Campà, R.G.; Bautista Pérez, L.; Félix de Castro, P. Plasma Technology Applied to Improve Wettability for Emerging Mycelium-Based Materials. *Processes* **2024**, *12*, 933. <https://doi.org/10.3390/pr12050933>

Academic Editors: Carles Corbella, Sabine Portal and Li Lin

Received: 22 March 2024

Revised: 23 April 2024

Accepted: 26 April 2024

Published: 3 May 2024



**Copyright:** © 2024 by the authors. Licensee MDPI, Basel, Switzerland. This article is an open access article distributed under the terms and conditions of the Creative Commons Attribution (CC BY) license (<https://creativecommons.org/licenses/by/4.0/>).

## 1. Introduction

The textile industry is one of the most polluting industries in the world, especially in terms of water consumption and land use. In 2020, all clothing, shoes and home textiles purchased by EU households required approximately 4000 m<sup>3</sup> m of blue water to be produced (inside and outside the EU), which is equivalent to 9 m<sup>3</sup> per person [1]. Moreover, the textile industry is estimated to be responsible for about 20% of global clean water pollution, wet processing of materials (dyeing, finishing, etc.) being the main cause of this huge consumption of water [2]. In this framework, plasma technology arises as a potential dry processing solution to reduce the amount of water used by the textile industry.

Plasma is the fourth state of matter and can be characterized as a mixture of partially ionized gases. The particles created within the plasma (atoms, radicals, ions and electrons, among others) possess high energy, which allows for the modification of surface chemical bonds without affecting bulk properties. It is an environmentally friendly technology that consumes a very low amount of chemicals and energy without any generation of wastewater [3]. Within the textile industry, plasma surface modification can be used in a variety of processes such as cleaning, activation, polymerization, etc. The main object of this study is to increase the material's wettability and enhance dyes' affinity by applying plasma treatments into novel mycelium-based materials. A textile's surface characteristics play a crucial role in its wetting properties, and by modifying the surface with plasma technology, these properties can be tailored in order to enhance their wettability and affinity towards other chemicals, such as dyes [4,5].

Mycelium-based materials are presented as emerging and sustainable flexible materials based on fungal mycelium. Mycelium is a characteristic structure, typical of fungi,

which grows in a dense network of ramified hyphae. These hyphae (which are filaments originating from fungi spores) are composed mainly of chitin, a long polymer chain of N-acetylglucosamine and chitosan, which is deacetylated chitin (Figure 1) [6]. Nevertheless, other structures are present on the mycelium cell wall, such as proteins (e.g., mannoproteins, hydrophobins) and glucans [7].

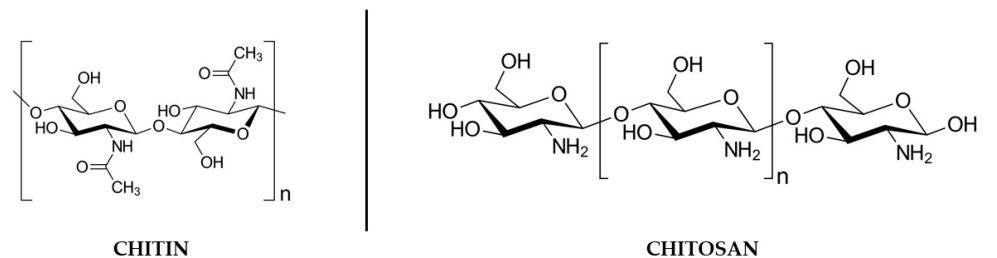


**Figure 1.** Chemical structures of chitin and chitosan.

Mycelium-based material stands out as a sustainable alternative to animal or synthetic leather, which present a higher environmental impact [8]. On the one hand, natural leather generates a large amount of toxic waste emissions, particularly from the tanning process, in which heavy metals, acids and dyes are employed [9]. Certainly, efficient depuration treatments of tanning processes have been developed, especially in developed countries; nonetheless a big part of leather production is carried out in countries where environmental regulations are less strict. On the other hand, synthetic leather is made of synthetic polymers (such as polyvinyl chloride or polyurethane), which, despite having a lower environmental impact than natural leather, can generate microplastics throughout their life cycle.

Therefore, the processing of mycelium materials to a final functional product is currently being studied. This research has been developed within this framework, by studying the plasma pre-treatment on this material in order to reduce the water, energy and chemicals consumption of the subsequent treatments, such as dyeing.

## 2. Materials and Methods

This research was focused on raw mycelium-based materials; therefore no other treatment was performed previously. The mycelium panels were produced and provided by MOGU S.R.L, an Italian company whose expertise is in mycelium and its derivative materials.

### 2.1. Plasma Treatments

Plasma treatments of raw mycelium-based materials were performed with a low-pressure plasma (LPP) Tetra-30-LF-PV (Diener Electronic GmbH). The equipment is shown in Figure 2. It consists of a vacuum plasma system with a 37 L capacity and a discharge source that operates at a low frequency (40 kHz) and at maximum power of discharge of 1.0 kW. Four trays are symmetrically placed between five planar electrodes, which are also arranged inside the chamber at a constant distance and connected to the low-frequency generator. Plasma was generated by direct-current glow discharge in air, with a constant gas flow rate (20 sccm) and at a pressure of 30 mbar. The working power applied between the electrodes under these conditions creates the needed energy to produce plasma.

In this case, the treatment was studied at several working powers (between 0 W and 1000 W) and treatment times (between 0 min and 30 min).

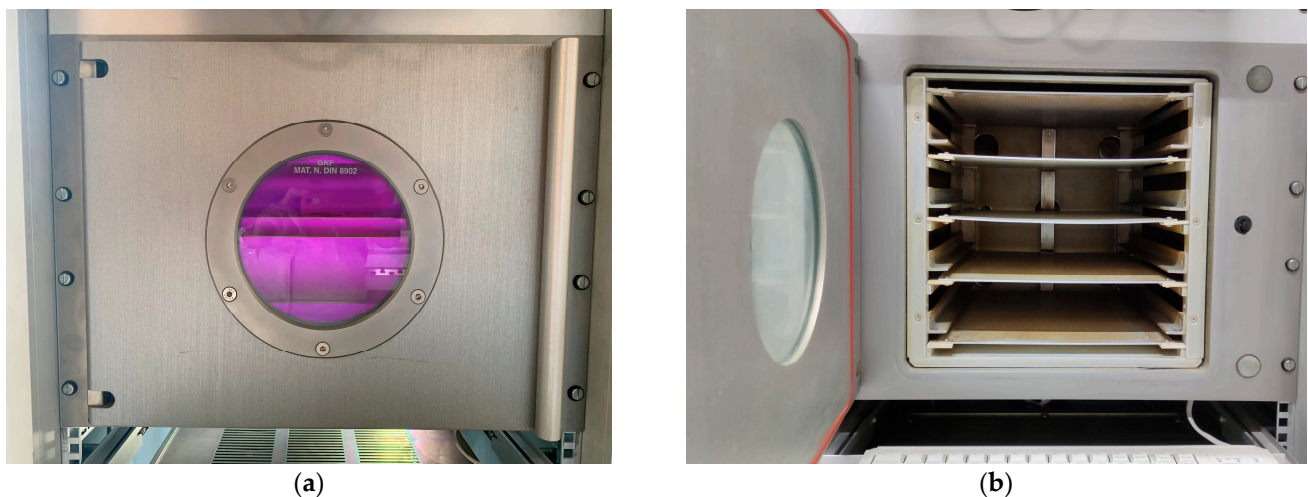


**Figure 2.** Low pressure plasma equipment (Diener Electronic GmbH). (a) Outside of the equipment, including the main screen and vacuum chamber door. (b) Vacuum chamber on the inside.

## 2.2. Characterization

### 2.2.1. Water Absorption and Water Contact Angle

Different properties related to the wetting and wicking of the mycelium-based material were measured. Wetting is related to the interaction between the solid surface and a specific liquid (as defined by E. Kissa [10], it is the displacement of a fiber–air interface with fiber–liquid interface) and has been assessed by measuring the WCA (water contact angle). Wicking is associated with the capillarity of a porous substrate and has been assessed by measuring the water absorption capacity. Nevertheless, since wetting influences the capillarity forces, wettability is considered a prerequisite of wicking [11].

The water absorption capacity of the mycelium-based materials was preliminarily assessed following UNE-EN ISO 9073-6 [12], a standardized procedure that sets the immersion time in water (1 min) and the draining time afterwards (2 min). Thus, the weight difference between the wet material (after 2 min of draining) and the dry material provides the information regarding the water absorption capacity (Equation (1)).

$$\text{Water absorption capacity (\%)} = \frac{\text{Weight}_f - \text{Weight}_o}{\text{Weight}_o} \cdot 100 \quad (1)$$

where  $\text{Weight}_f$  = weight of the sample after draining the material for two minutes;  $\text{Weight}_o$  = initial weight of the sample (dry).

In order to evaluate the WCA and water absorption capacity properties of the mycelium, a Krüss K100 MK2 tensiometer was employed (see Figure 3), following the Washburn method, which is indicated for porous hydrophilic materials (WCA lower than  $90^\circ$ ). In this model, WCA is measured by using the capillary forces previously measured and the following Equation (2) [13].

$$\frac{m^2}{t} = \frac{c \cdot \rho^2 \cdot \sigma \cdot \cos \theta}{\eta} \quad (2)$$

where  $m$  = mass;  $t$  = flow time;  $\sigma$  = surface tension of the liquid;  $c$  = capillary constant of the sample;  $\rho$  = density of the liquid;  $\theta$  = contact angle;  $\eta$  = viscosity of the liquid.

Another crucial parameter that can be obtained with this model is the water absorption capacity (%), considering the weight of the sample (2 cm × 2 cm) before the measurement and the weight of water absorbed by the sample after a certain period of time. In this case, the absorption capacity was measured at 500 s, which is the elapsed time since the first contact with the liquid (water).

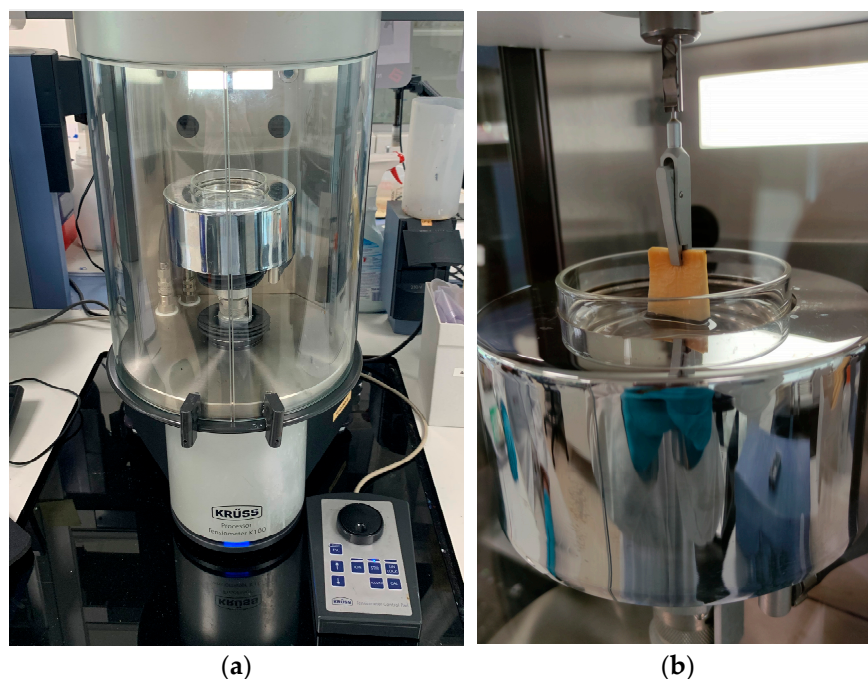


**Figure 3.** (a) Tensiometer (Krüss K100 MK2). (b) Set-up for measuring WCA and water absorption capacity of mycelium-based material.

### 2.2.2. SEM

The characterization of the surface of the mycelium samples was performed using Scanning Electron Microscopy (SEM). The equipment employed was SEM TOUCHSCOPE JEOL JSM-6010LV, from JEOL INSTRUMENTS (Tokyo, Japan) and the beam of electrons is produced by a Tungsten (W) filament.

Images were taken with Secondary Electrons Image (SEI) mode and samples were previously coated with a nanometric layer of a metal. In this case the metallization is performed with a CRESSINGTON SCIENTIFIC SPUTTER COATER (108AUTO), from Cressington Scientific Instruments (Watfor, UK) with a gold (Au) target. By sputtering the sample for 30 s, a gold coating of 6–10 nm thickness is obtained.

### 2.2.3. XPS

X-Ray photoelectron spectroscopy (XPS) is a broadly used characterization technique to analyze the surface elemental composition and their chemical state. The technique is based on the photoelectric effect, which is achieved with the irradiation of the material with a beam of X-rays, and it can measure the surface of a material through its first nanometers (~10 nm) [14].

Mycelium samples were placed on the holders with carbon tape, and this was left in the vacuum chamber overnight and analyzed within the next 24 h.

The XPS characterization of the mycelium samples was performed in a SPECS system with a PHOIBOS 150 EP hemispherical energy analyzer with MCD-9 detector, from SPECS Surface Nano Analysis GmbH (Berlin, Germany) at a pressure of approximately  $1 \times 10^{-8}$  mbar. The X-ray source employed was an XR-50 Al Kalfa line of 1486.6 eV energy, placed at 54.7 degrees respect to the analyzer axis. A survey spectrum was acquired at 200 W power and using a pass energy of 30 eV, with a dwell time of 0.1 s and an energy step of 1 eV. High-resolution spectra were acquired at 200 W and a pass energy of 20 eV, with a dwell time of 0.25 s and an energy step of 0.1 eV.

The detector was calibrated by the 3d5/2 line of Ag with a full width at half maximum (FWHM) of 1.211 eV.



### 2.3. Design Expert 13 (Software)

The optimization of the processes was developed with the assistance of the software program Design Expert 13, which is a powerful statistical tool for the design of experiments (DOE). The response surface methodology was employed to model an equation and determine the optimum parameters in each case [15].

For the final plasma treatment optimization, an “aleatory range” was selected and 17 experiments were conducted under different powers (between 0 W and 1000 W) and times (between 0 min and 30 min). The chosen responses were absorption velocity ( $\text{g}^2/\text{s}$ ) and absorption capacity (%), which were measured with the tensiometer.

### 2.4. Dyeing Process

In order to evaluate the dye penetration inside the mycelium material, a dyeing protocol was defined. To perform the dyeing, an infrared heat assisted laboratory dyeing machine was employed (Redkrome RED P, from UGOLINI (Schio, Italy)), using individual vessels of approximately 250 mL capacity (Figure 4).



**Figure 4.** Infrared heat assisted dyeing machine (Redkrome RED P, Ugolini).

The dyeing protocol consists of using 1% w.o.f. dye (using Isolan Black Dystar<sup>®</sup> as acid dye or Astrazon Red<sup>®</sup> as basic dye), 20% w.o.f. fat liquoring and 10% w.o.f NaCl in the dyeing bath, using a 1:30 MLR (mass:liquor ratio). The dyeing bath and the sample are put inside the vessel, which is then placed inside the laboratory dyeing machine. Then, the dyeing program is adjusted to have a 60 min dyeing process, at 50 °C, with a heating rate of 1.5 °C/min.

## 3. Results and Discussion

### 3.1. Plasma Treatment Optimization

An optimization study of the low-pressure plasma treatment on raw mycelium panels was performed, so that the best conditions for an optimal performance in terms of wettability could be defined.

Nevertheless, to pave the way for the study, some previous analyses were performed beforehand to observe the behavior of mycelium towards plasma treatments. For instance, regarding water absorption capacity (UNE-EN ISO 9073-6) [12], mycelium material obtained a water absorption (%) of 73%, whereas with a plasma treatment of 900 W and 30 min, this value was increased to 1776%, showing that plasma improves the water absorption capacity of the material. On the other hand, it was observed that, when treated with plasma, the thickness of the mycelium material changed drastically after submerging it in water (wet-processing). That effect was not observed in non-treated mycelium samples, which could indicate that plasma might be creating soluble functional groups.

Finally, another issue that was detected with mycelium was the poor penetration of dyeing and finishing formulations. Some preliminary dyeing processes were performed,

with acidic and basic dyes, and the cross-section was evaluated. As can be seen in Figure 5, the cross-section of mycelium-based materials is hardly dyed when no plasma is applied, which is in line with the results obtained regarding water absorption capacity; the higher the absorption capacity, the higher the dye uptake, and therefore, it is more likely to penetrate the mycelium core. Figure 5 shows the thickness variation produced after a wet processing, this effect being particularly noteworthy on plasma treated samples.

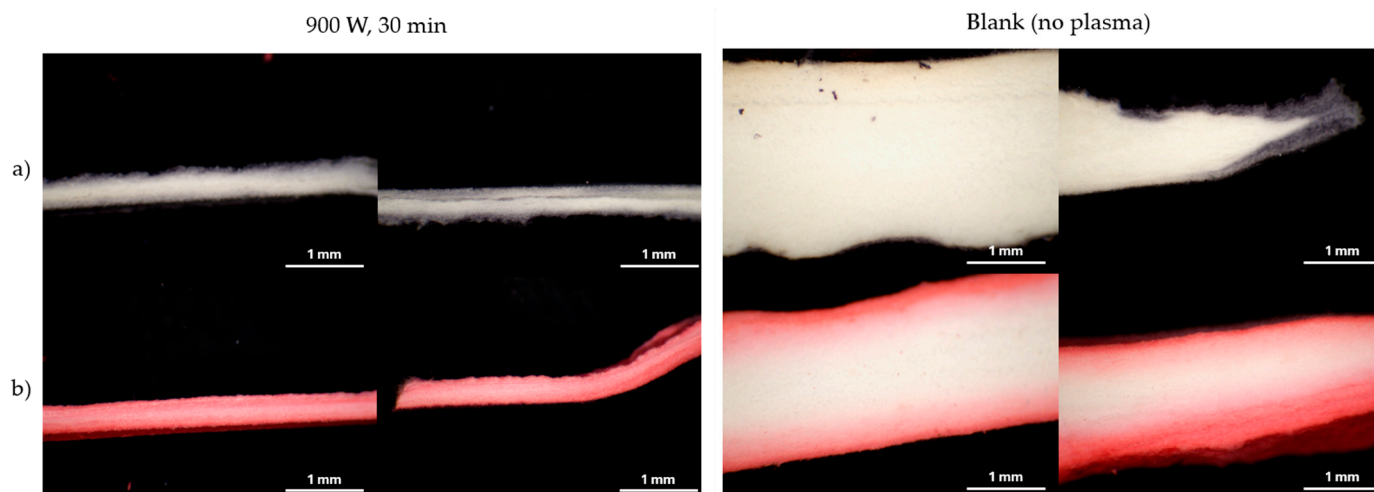


**Figure 5.** Cross-section of dyed mycelium panels. Samples were dyed with (a) acidic dye (Isolan Black Dystar®) and (b) basic dye (Astrazon Red®). Pictures were taken with the same magnification.

Once the mycelium material had been preliminarily studied after low pressure plasma (LPP) treatments, an optimization experimental plan was prepared with the assistance of Design Expert 13, and the complete plan and results are summarized in Appendix A (Table A1). As can be seen, three different responses were selected: absorption capacity (%) and absorption velocity ( $\text{g}^2/\text{s}$ ) and water contact angle (WCA, °). Those parameters were measured with the tensiometer by applying the Washburn method. Nevertheless, plasma-treated samples showed a WCA value of  $0^\circ$ , except for samples treated for 1 min, at 10 W ( $85.78^\circ$ ) and 420 W ( $73.84^\circ$ ). On the other hand, for raw material, a WCA of almost  $90^\circ$  was observed ( $89.88^\circ$ ). This is why WCA values were not considered for this optimization, since no significant variation was observed for plasma-treated samples.

To sum up, absorption capacity and absorption velocity results (Table A1, Appendix A) corroborate the increased wicking properties with plasma treatment, while the raw mycelium material reached a value of 103% (at 500 s) and  $0.00139 \text{ g}^2/\text{s}$ . The trends followed by the two parameters are easier to follow on the surface response graphs produced by the statistical analysis performed in Design Expert 13, which are shown in Figure 6. In this case, an inflexion point is obtained for both parameters (power and time): higher times and powers do not imply a higher absorption capacity.

As explained in the bibliography, plasma could be introducing hydrophilic groups onto treated surfaces via oxidation (e.g., carbonyl, carboxyl or hydroxyl groups) [5]. Nevertheless, with mycelium-based material, higher oxidation (higher times and powers) does not imply higher water absorption, as the results show. For instance, it could be that less oxidated samples maintain more hydroxyl groups, which are highly hydrophilic, whereas a plasma overtreatment could further oxidize those hydroxyl groups, thus obtaining carbonyl or carboxyl groups, which are not as hydrophilic. Nevertheless, this hypothesis will be discarded with the XPS results.

With the optimization tool that Design Expert 13 brings, the statistical model can be analyzed in hypothetical scenarios. Optimizing the plasma treatment, in this case, meant lowering power and time to reduce consumption, while obtaining good absorption properties. Finally, the optimized parameters found were 17.5 min at 750 W of power.

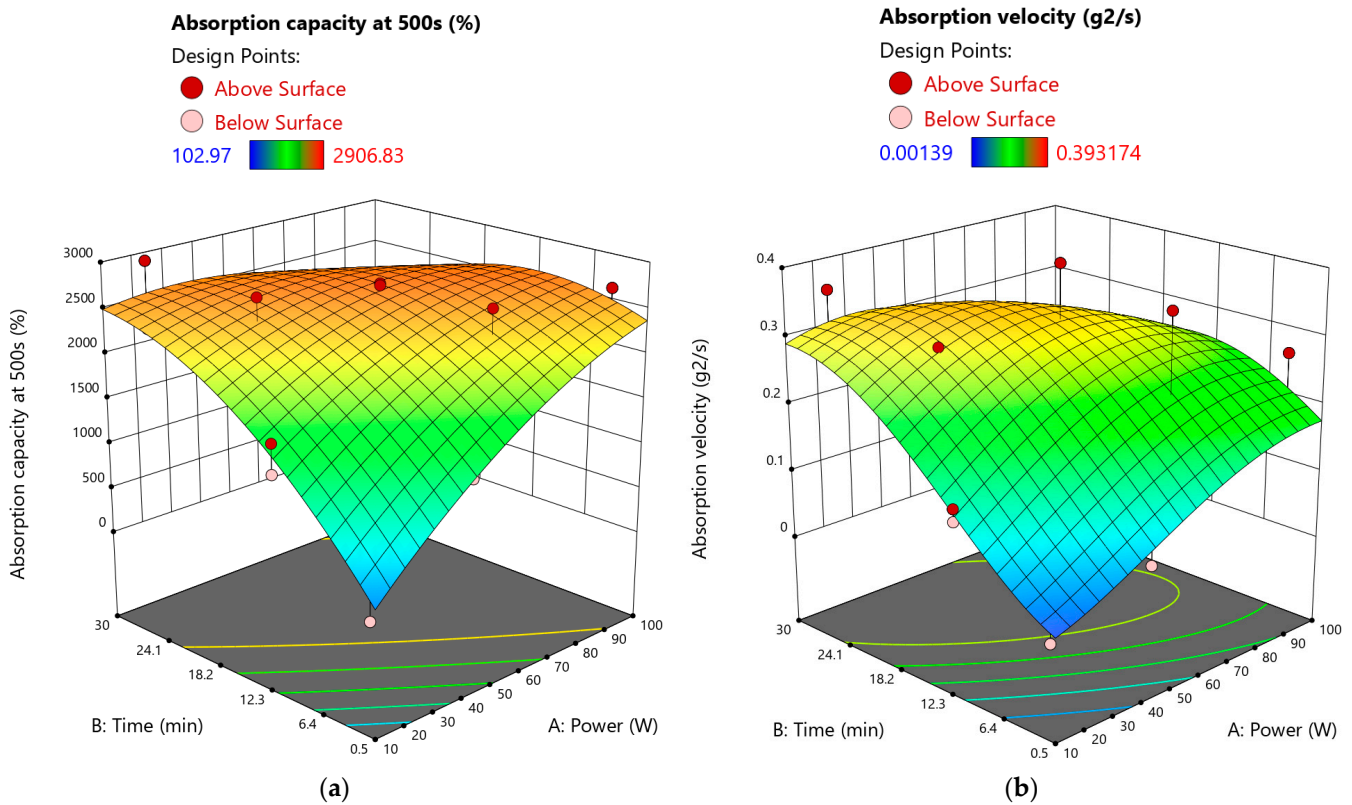


**Figure 6.** Surface response graphs after the study at different plasma conditions (time and power): (a) absorption capacity at 500 s, (b) absorption velocity. The red and pink dots correspond to the experiment design points, which obtained results are above and below the generated surface response, respectively.

### 3.2. Plasma Ageing (Stability over Time)

Another interesting factor to assess is the stability of the plasma treatment over time, considering wettability (WCA) and water absorption capacity. To do so, mycelium samples were treated with the optimal conditions (750 W and 17.5 min), and then the behavior of the material was tracked over time (0, 3, 10, 20, 30 and 60 days) by measuring with the tensiometer their absorption capacity (at 500 s) and WCA.

Regarding WCA results, as showed in the previous section, the values obtained for plasma-treated samples were  $0^\circ$ , and therefore no variation in values could be observed. On the other hand, the results for water absorption capacity are represented in Figure 7, but numerical data are summarized on Appendix A (Table A1). Regarding the stability of the plasma treatment, it is shown that the absorption capacity after 58 days (2080%) slightly decreases but remains almost the same as on the first day of the treatment (2400%). This indicates that some kind of permanent oxidation could be occurring in the mycelium's surface. To further comprehend the effect of plasma in mycelium-based materials, surface characterization has been performed. Nonetheless, these are promising results, since typically plasma surface activation lasts for some minutes to several weeks. This long-lasting effect will be highly beneficial in possible upcoming industrialization.

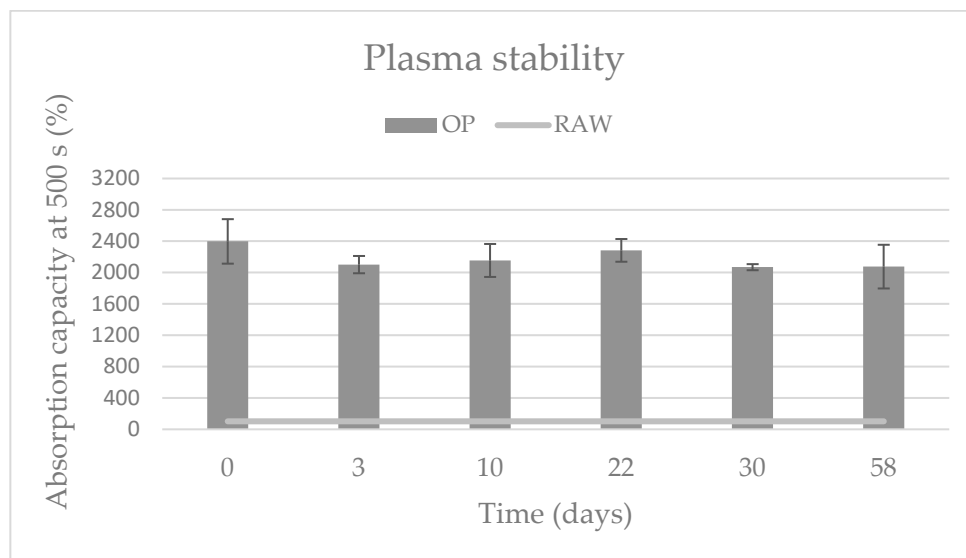


**Figure 7.** Absorption capacity (%) of plasma-treated mycelium material over time.

### 3.3. Characterization of Mycelium Surface after Plasma Treatment

To better understand the effect of plasma treatment on the surface of mycelium-based materials, different characterization techniques were used, such as scanning electron microscopy (SEM) and X-ray photoelectron spectroscopy (XPS). In Table 1, there is a legend of the different samples that were analyzed:

**Table 1.** Samples characterized by XPS analysis (code names, sample characteristics and plasma treatment conditions).

Code Name	Sample	Plasma Conditions
RAW	Untreated	-
OP	Optimal plasma treatment	750 W and 17.5 min
OV	Overtreated	1000 W and 30 min

#### 3.3.1. SEM

SEM images were captured for both faces of the mycelium, since it grows vertically from the substrate (mycelium biomass). In the case of the top layer, slight surface differences are observed with plasma treatments. Furthermore, the overtreated mycelium showed some surface degradation, and some modifications began to appear within the fibers of the material, especially on the top layer (Figure 8). These observations are in line with the results obtained for water absorption, since when the plasma treatment is too aggressive, the material can be damaged, and as a result, the water absorption is decreased or not further increased.

As suggested by I.B. Khalifa et al., a phenomenon called ablation could happen when atmospheric air plasma treatment is too energetic, contributing to the removal of the hydrophilic functional groups [16]. As seen in the images, a similar phenomenon could be happening on the overtreated samples, damaging the material and obtaining a decrease (or not further increase) in the absorption capacity.



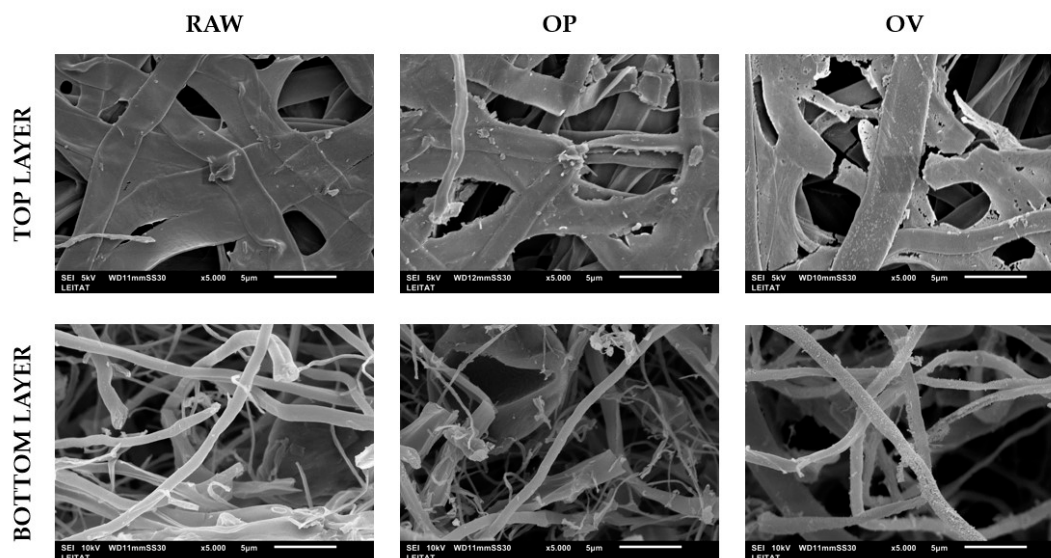


**Figure 8.** SEM images of mycelium samples with different plasma treatments (magnification  $\times 5000$ ).

### 3.3.2. XPS

Due to the irregularity of the mycelium material, the XPS analysis was performed on different mycelium panels. Therefore, for each condition (Raw, OP, OV), 3 different mycelium panels were treated and analyzed.

The spectra obtained from the XPS analysis of the 3 different references (RAW, OP, OV) are summarized in Appendix B (Figures A1–A3 respectively). The main peaks of each sample are O1s ( $\sim 532$  eV), N1s ( $\sim 400$  eV) and C1s ( $\sim 285$  eV), which corresponds to the expected elemental constitution for mycelium, whose structure is mainly made of chitin, chitosan, glucans and proteins. To more easily perceive the quantified differences between samples, the obtained atomic concentrations are represented in a bar chart (see Figure 9a). Numeric data are shown in Appendix A (Table A3). Nevertheless, other peaks are also present in the samples, such as Na, K, Mg, Ca, P and S, which can be attributed to contamination due to sample manipulation, or even Fe, Zn and Cr, which can be attributed to the sample holder, which was made of stainless steel.

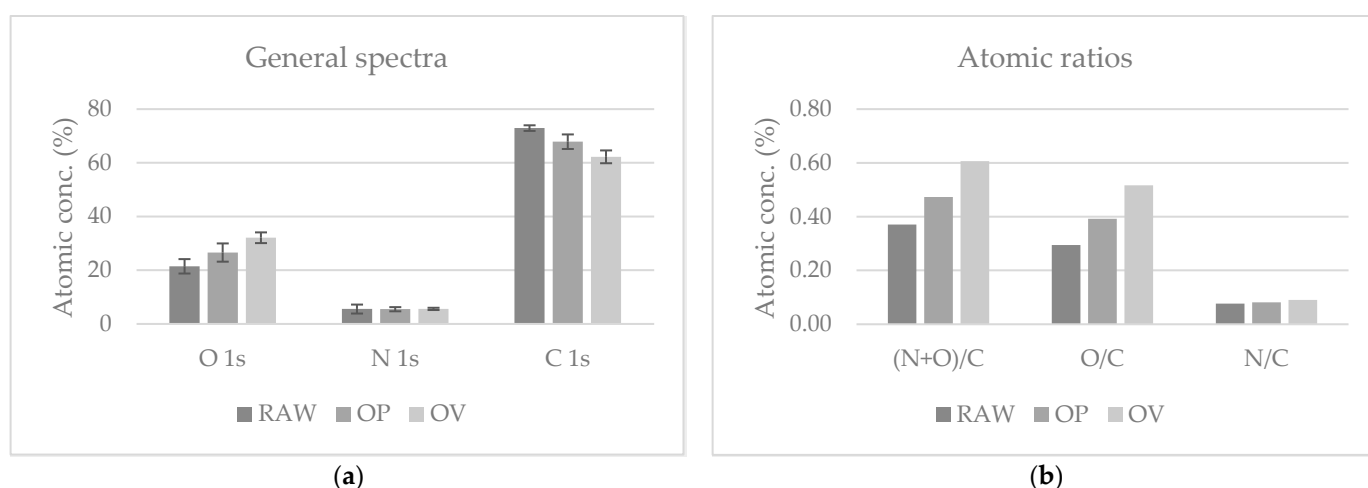


**Figure 9.** XPS general spectra results of mycelium samples with different plasma treatments: (a) Atomic concentrations (%). (b) Atomic ratios.

Regarding the results from the general spectra of the mycelium, it is observed how the surface atomic concentration of oxygen increases, since the plasma treatment increases the hydrophilicity by introducing polar functional groups. This effect on the surface atomic

concentration is in line with the obtained results on water absorption capacity. On the other hand, the spectra show no significant variation in nitrogen concentration, and carbon content is decreased when plasma is applied. The fact that carbon content is reduced with plasma treatment discards the assumption made on the previous section about the higher presence of carboxyl groups on overtreated samples.

Furthermore, atomic ratios have been calculated from the data obtained in the general spectra (see Figure 9b). It is easily detected that the higher the intensity of the plasma treatment, the higher the ratios with respect to carbon, although O/C increases at a higher ratio than N/C with plasma treatment intensity. Despite the general spectra showing no significant variation in N content (%), the N/C atomic ratio shows that the higher the energy of the plasma treatment, the higher the N/C ratio. Therefore, more carbon is being removed than nitrogen.

To sum up, the mycelium-based material has several chemical structures within its surface, such as chitin, chitosan, glucan or proteins, and plasma treatment is expected to modify those that are present in the surface (breaking of bonds, recombination, electron promotion, etc.), increasing the hydrophilicity. Plasma irradiation can cause the breaking of the glycosidic bonds or even of the carbon bonds of the chitin chain, and oxidation of the formed free radicals could also be occurring. Moreover, the modification of the glucan structure or the outer layer of proteins can also be occurring, such as the protein hydrophobin, which can form a hydrophobic layer on the mycelium surface [7]. The modification of this protein could lead to a loss in carbon content as well as a decrease in hydrophobicity, until an inflexion point is reached, where the plasma treatment could start producing the so-called ablation and removal of the hydrophilic groups. This ablation or etching was already observed on SEM images.

Additionally, the analysis of the C1s high-definition spectrum was also performed, for a qualitative interpretation. The spectra for the RAW, OP and OV samples are shown in Figures 10a, 10b and 10c, respectively, where the intensity (CPS, counts per second) has been normalized for facilitating the interpretation.

As was previously commented, 3 different panels were analyzed due to the high irregularity of the mycelium-based material. This variability is shown in the high-definition spectra, where some peaks outside the C1s binding energy (285 eV) appear for just some of the replicates (in either case the three of them). This fact hinders the accurate interpretation of the XPS spectra.

One thing in common among the three different spectra (RAW, OP and OV), is the appearance of two peaks: one around 285 eV, which corresponds to C1s, and another around 282 eV, which according to the bibliography can be attributed to metal carbides [17]. It can be seen how, in raw samples, the first peak (285 eV) is wider, meaning that among 290–284 eV, the number of chemical species based on carbon is higher. This is in line with the results shown in the general spectrum, where raw material obtained the highest C1s atomic concentration.

On the other hand, plasma-treated samples (OP and OV) obtain an additional peak at around 293 eV. According to bibliography, it can be attributed to K2p [18]. When analyzing the general spectra, one of the new peaks that appeared on plasma-treated samples was a peak around 377 eV, which could confirm the potassium presence, since K2s binding energy is around 378 eV. Also, the normalized intensity of this peak (~293 eV), is higher in OV samples (0.37 CPS) than OP samples (0.23 CPS), which could mean that the higher the plasma intensity, the higher the potassium content on the material surface, which could indicate some kind of ablation of the outside layer of the mycelium.

The analysis of XPS is usually challenging, but even more so in this case, with an unknown and chemically complex material such as mycelium. This material is produced through a biological process, where it is difficult to control the characteristics of the resultant products, like thickness, density or even texture. Although the plasma effect should be homogeneous within the surface of the material, the irregularity of the material resulted

in different plasma effects in different regions within the same sample, or even between different samples treated under the same conditions.

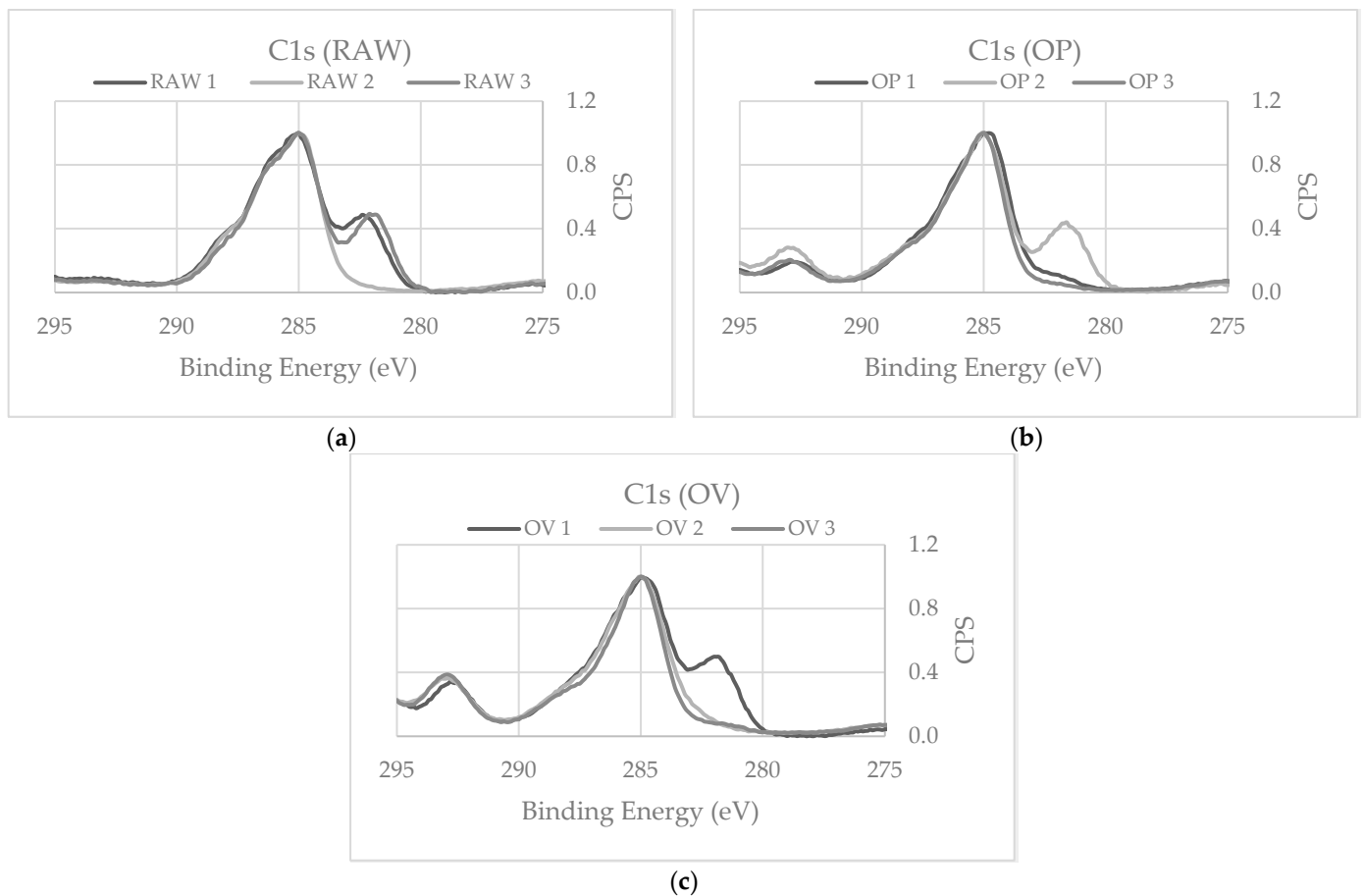


**Figure 10.** XPS C1s high-definition spectra of mycelium samples with different plasma treatments: (a) Raw. (b) Optimal plasma. (c) Overtreated plasma.

#### 4. Conclusions

In this research, several topics have been studied regarding mycelium, plasma technology and its characterization.

On the one hand, a new and emergent material such as mycelium has been successfully treated with plasma technology. The plasma process has been optimized to maximize the outcome (wettability and water absorption capacity) while reducing the energy consumption (discharge power and treatment time), resulting in a lower environmental impact and higher efficiency. The optimal plasma treatment for this material was found to be 750 W and 17.5 min, obtaining an increase of more than 2000% in water absorption capacity.

On the other hand, several efforts have been made to characterize and understand the effect of plasma treatments within this emerging material. Besides the hydrophilic properties obtained with the plasma treatment, other aspects were studied to fully characterize the treated mycelium-based materials. For instance, SEM was employed to visually evaluate possible etching or modifications on the morphology of mycelium fibres. No significant differences were observed; nonetheless, when higher energies were applied (overtreated samples), some damage began to appear on mycelium panels, especially on the top layer. Moreover, XPS analysis confirmed that chemical modifications were being made, when comparing the general and high-resolution spectra obtained for raw and plasma-treated samples. The results of both characterization methods suggest that plasma treatment causes the chemical modification of mycelium surface (i.e., some surface proteins, such as

hydrophobin), and for more intense plasma treatments, the so-called ablation phenomenon appeared, thus achieving worse wettability.

Nevertheless, more research is still needed for better understanding of the influence of plasma treatments on physicochemical modifications of mycelium-based materials.

**Author Contributions:** Conceptualization, P.A.C., N.P.G., R.G.C., L.B.P. and P.F.d.C.; methodology, P.A.C., N.P.G., R.G.C., L.B.P. and P.F.d.C.; validation, P.A.C., N.P.G., R.G.C., L.B.P. and P.F.d.C.; formal analysis, P.A.C. and N.P.G.; investigation, P.A.C. and N.P.G.; data curation, P.A.C. and N.P.G.; writing—original draft preparation, P.A.C.; writing—review and editing, P.A.C., N.P.G., R.G.C., L.B.P. and P.F.d.C.; visualization, P.A.C.; supervision, R.G.C., L.B.P. and P.F.d.C.; project administration, R.G.C., L.B.P. and P.F.d.C. All authors have read and agreed to the published version of the manuscript.

**Funding:** This research has received funding from the European Union’s Horizon 2020 research and innovation programme under grant agreement No. 101000719.

**Data Availability Statement:** The original contributions presented in the study are included in the article, further inquiries can be directed to the corresponding author.

**Acknowledgments:** To Centre de Recerca en Ciència i Enginyeria Multiescala de Barcelona (Universitat Politècnica de Catalunya), who performed the XPS analysis and gave support with the interpretation of the obtained data.

**Conflicts of Interest:** The authors declare no conflicts of interest. The funders had no role in the design of the study; in the collection, analyses, or interpretation of data; in the writing of the manuscript; or in the decision to publish the results.

## Appendix A

In this appendix, tables with supplementary data regarding the graphics utilized on this article are shown.

Table A1 shows the absorption velocity and the absorption capacity results for the plasma treatment optimization performed with Design Expert 13, which are discussed on Section 3.1.

**Table A1.** Summarized values of the results for the “aleatory range” DoE plasma treatment optimization on mycelium-based materials. Contact angle (CA) results were not taken under consideration for the optimization process with Design Expert software.

Power (W)	Time (min)	Contact Angle (°)	Absorption Velocity (g <sup>2</sup> /h)	Absorption Capacity at 500 s (%)
0	0	89.88	5	103
100	1	85.78	19	225
100	11	0	434	1672
100	11	0	500	1348
230	30	0	978	2161
230	30	0	1273	2907
310	20	0	1071	2709
420	1	73.84	199	1287
610	30	0	633	2301
620	17	0	1415	2667
620	17	0	966	2434
620	17	0	1085	2645
680	7	0	1272	2616
1000	4	0	948	2429
1000	4	0	600	2633
1000	17	0	461	2275
1000	30	0	789	2124

Table A2 shows the absorption capacity over time of plasma-treated mycelium (with the optimal conditions; 17.5 min and 750 W). These data are represented in the results section (Figure 7).



**Table A2.** Summary of absorption capacity (%) of plasma-treated mycelium over time.

Days	Absorption Capacity (%)
RAW	100 ± 30
0	2400 ± 280
3	2100 ± 110
10	2160 ± 210
22	2280 ± 100
30	2070 ± 40
58	2080 ± 280

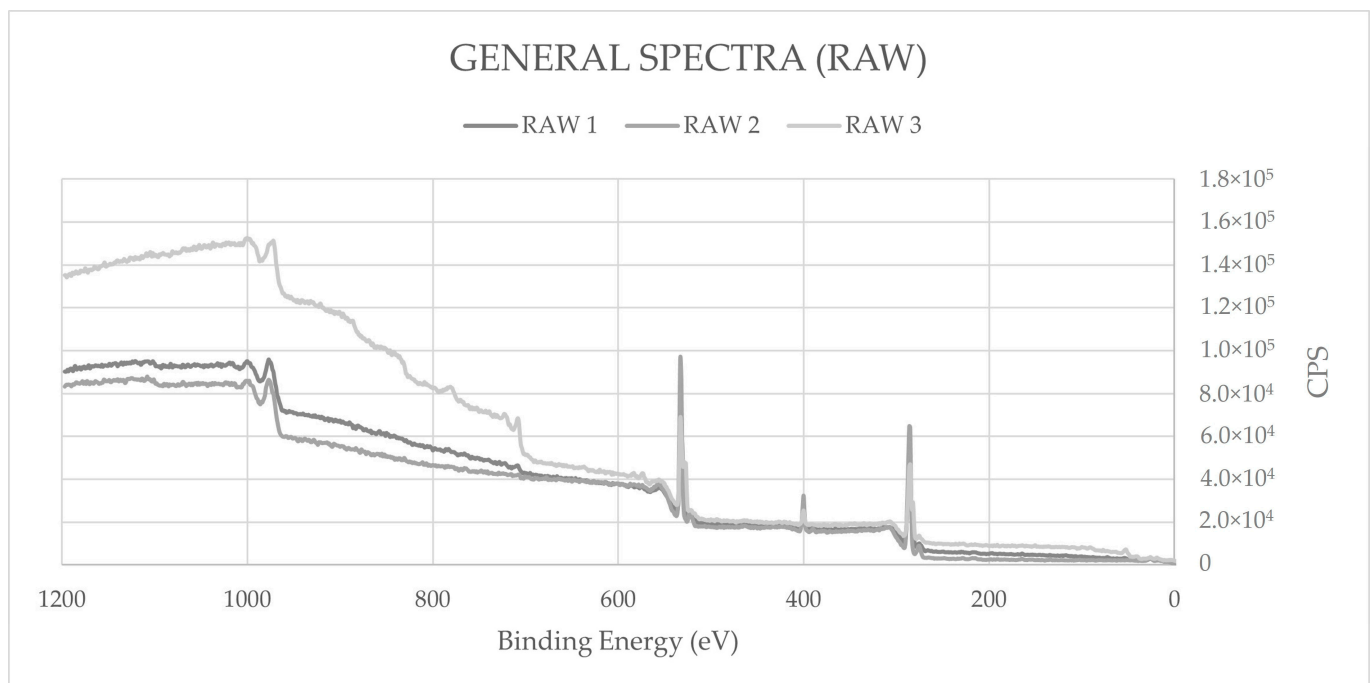
Table A3 shows the atomic concentration (%) numeric values of the XPS analysis, which are also represented in a bar graph on the results section (Figure 9a).

**Table A3.** Summary of the atomic concentration (%) values obtained from the XPS general spectra analysis of mycelium references with different plasma treatments.

	O1s	N1s	C1s
	At. Conc %	At. Conc %	At. Conc %
RAW	21.5 ± 2.7	5.6 ± 1.7	72.9 ± 1.0
OP	27 ± 3	5.5 ± 0.8	67.9 ± 2.7
OV	32.1 ± 2.0	5.6 ± 0.4	62.2 ± 2.4

## Appendix B

In this appendix, general spectra for the Raw, Optimal and Overtreated mycelium samples are shown (Figures A1–A3 respectively).

**Figure A1.** XPS general spectra for raw mycelium-based materials.

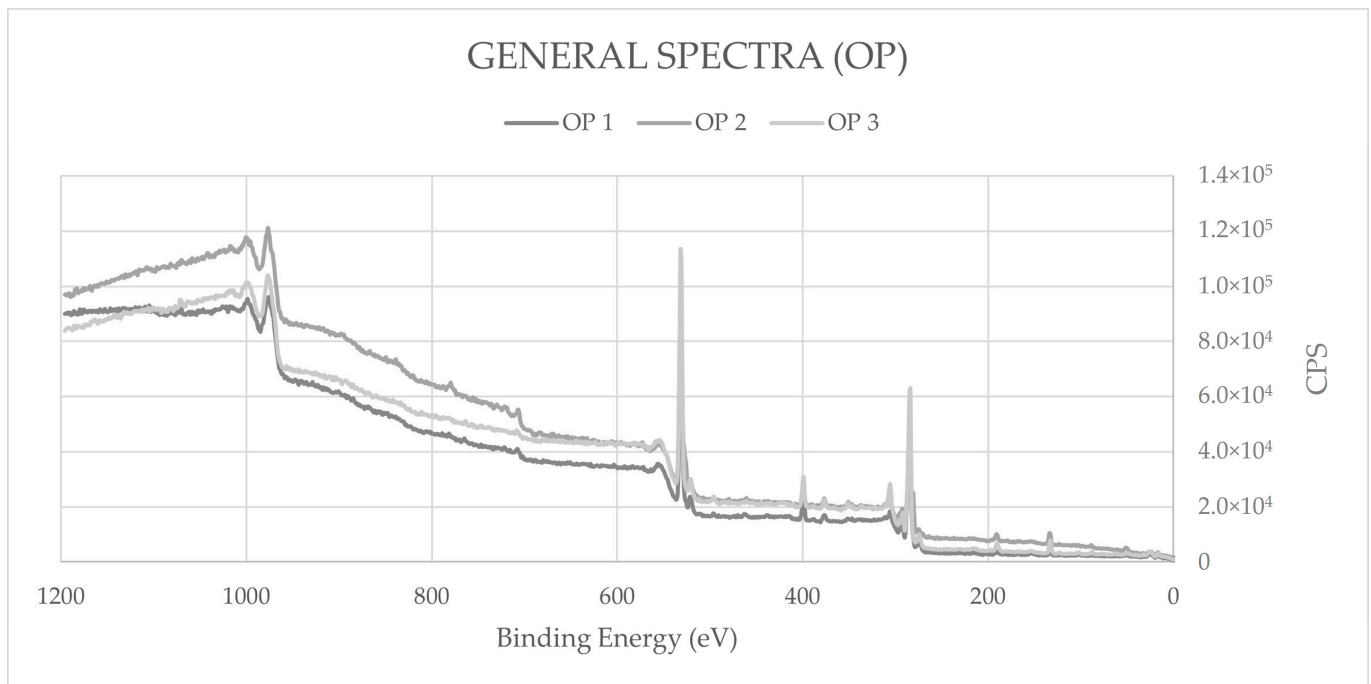


Figure A2. XPS general spectra for optimal plasma-treated mycelium-based materials.

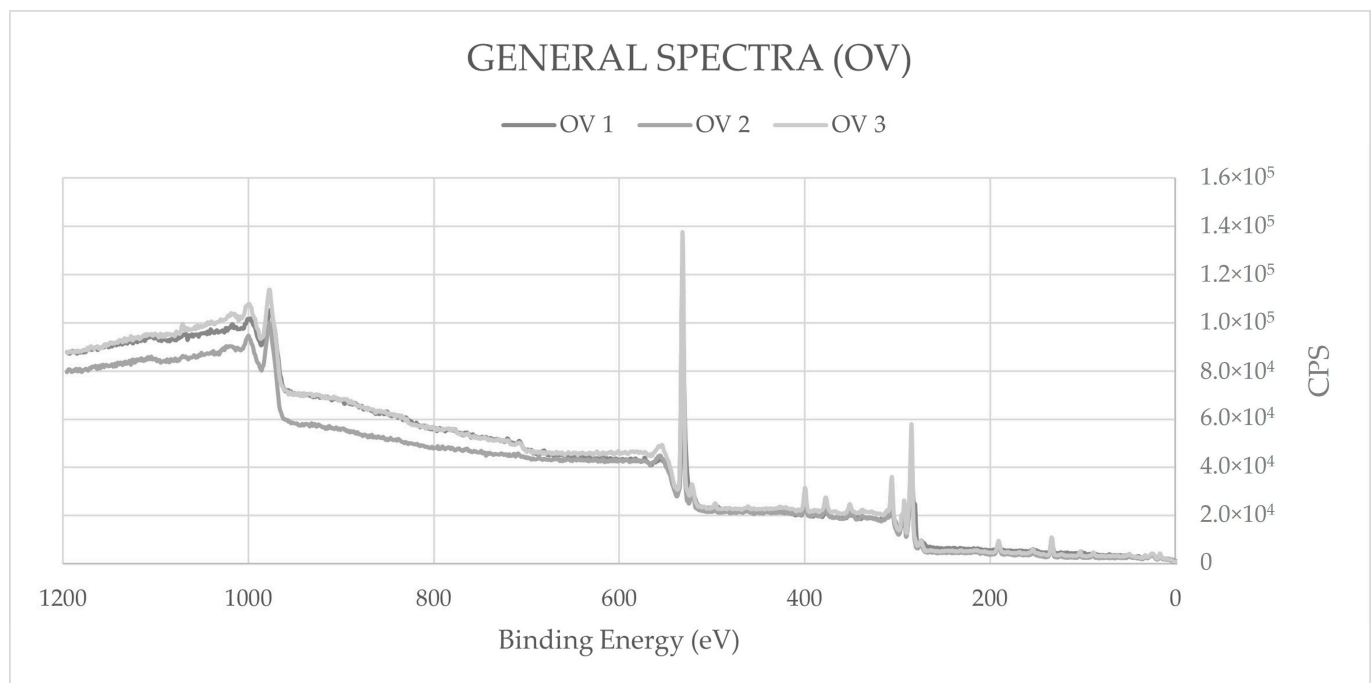


Figure A3. XPS general spectra for overtreated mycelium-based materials.

## References

1. Textiles and the Environment: The Role of Design in Europe's Circular Economy. [Online]. Available online: <https://www.eea.europa.eu/publications/textiles-and-the-environment-the/textiles-and-the-environment-the> (accessed on 15 January 2024).
2. The Impact of Textile Production and Waste on the Environment (Infographics)'. [Online]. Available online: <https://www.europarl.europa.eu/news/en/headlines/society/20201208STO93327/the-impact-of-textile-production-and-waste-on-the-environment-infographics#:~:text=Textile%20production%20is%20estimated%20to,microplastics%20released%20into%20the%20environment> (accessed on 15 January 2024).
3. Bautista, L.; Paul, R.; Mota, J.; DelaVarga, M.; Garrido-Franco, M.; Aubouy, L.; Briz, A.; de la Ossa, P.P. Dyeing of low-pressure oxygen-plasma treated wool fabrics with antibacterial natural dyes. *Int. Dye* **2007**, *192*, 14+16+18+20.

4. Hasanbeigi, A.; Price, L. A technical review of emerging technologies for energy and water efficiency and pollution reduction in the textile industry. *J. Clean. Prod.* **2015**, *95*, 30–44. [[CrossRef](#)]
5. Haji, A.; Naebe, M. Cleaner dyeing of textiles using plasma treatment and natural dyes: A review. *J. Clean. Prod.* **2020**, *265*, 121866. [[CrossRef](#)]
6. Gow, N.A.R.; Latge, J.-P.; Munro, C.A. The Fungal Cell Wall: Structure, Biosynthesis, and Function. *Microbiol. Spectr.* **2017**, *5*, 5.3.01. [[CrossRef](#)]
7. Haneef, M.; Ceseracciu, L.; Canale, C.; Bayer, I.S.; Heredia-Guerrero, J.A.; Athanassiou, A. Advanced Materials From Fungal Mycelium: Fabrication and Tuning of Physical Properties. *Sci. Rep.* **2017**, *7*, 41292. [[CrossRef](#)] [[PubMed](#)]
8. Amobonye, A.; Lalung, J.; Awasthi, M.K.; Pillai, S. Fungal mycelium as leather alternative: A sustainable biogenic material for the fashion industry. *Sustain. Mater. Technol.* **2023**, *38*, e00724. [[CrossRef](#)]
9. Junaid, M.; Hashmi, M.Z.; Tang, Y.-M.; Malik, R.N.; Pei, D.-S. Potential health risk of heavy metals in the leather manufacturing industries in Sialkot, Pakistan. *Sci. Rep.* **2017**, *7*, 8848. [[CrossRef](#)] [[PubMed](#)]
10. Kissa, E. Wetting and Wicking. *Text. Res. J.* **1996**, *66*, 660–668. [[CrossRef](#)]
11. Patnaik, A.; Rengasamy, R.S.; Kothari, V.K.; Ghosh, A. Wetting and Wicking in Fibrous Materials. *Text. Prog.* **2006**, *38*, 1–105. [[CrossRef](#)]
12. UNE-EN ISO 9073-6:2003; Textiles—Test Methods for Nonwovens—Part 6: Absorption. European Committee for Standardization: Brussels, Belgium, 2003.
13. Washburn, E.W. The Dynamics of Capillary Flow. *Phys. Rev.* **1921**, *17*, 273–283. [[CrossRef](#)]
14. Aguilar, Z.P. Types of Nanomaterials and Corresponding Methods of Synthesis. In *Nanomaterials for Medical Applications*; Elsevier: Amsterdam, The Netherlands, 2013; pp. 33–82. [[CrossRef](#)]
15. Bezerra, M.A.; Santelli, R.E.; Oliveira, E.P.; Villar, L.S.; Escalera, L.A. Response surface methodology (RSM) as a tool for optimization in analytical chemistry. *Talanta* **2008**, *76*, 965–977. [[CrossRef](#)] [[PubMed](#)]
16. Khalifa, I.B.; Ladhari, N. Hydrophobic behavior of cotton fabric activated with air atmospheric-pressure plasma. *J. Text. Inst.* **2020**, *111*, 1191–1197. [[CrossRef](#)]
17. ‘Carbon XPS Analysis’, Cardiff University. [Online]. Available online: <https://sites.cardiff.ac.uk/xpsaccess/reference/carbon/> (accessed on 22 March 2024).
18. Potassium X-ray Photoelectron Spectra, Potassium Electron Configuration, and Other Elemental Information. Thermo Fisher Scientific. [Online]. Available online: <https://www.thermofisher.com/es/es/home/materials-science/learning-center/periodic-table/alkali-metal/potassium.html> (accessed on 22 February 2024).

**Disclaimer/Publisher’s Note:** The statements, opinions and data contained in all publications are solely those of the individual author(s) and contributor(s) and not of MDPI and/or the editor(s). MDPI and/or the editor(s) disclaim responsibility for any injury to people or property resulting from any ideas, methods, instructions or products referred to in the content.